

# Manganese Furnace Dust: Drying and Reduction of Zinc Oxide by Tar

Tasuku HAMANO,<sup>1)</sup> Guangqing ZHANG,<sup>1)</sup> Peter BROWN<sup>2)</sup> and Oleg OSTROVSKI<sup>1)</sup>

1) School of Materials Science and Engineering, University of New South Wales, UNSW Sydney, NSW 2052, Australia.

2) Tasmanian Electro Metallurgical Company Pty Ltd., TEMCO Road, Bell Bay, TAS 7253, Australia.

(Received on January 17, 2008; accepted on April 17, 2008)

Manganese furnace dust collected in smelting of manganese alloys is in the form of a slurry containing oxides of manganese, iron, zinc and other metals, and tar. Drying of manganese furnace dust and removing zinc from the dust are essential steps to recycle the dust to the smelting furnaces. This paper presents results of drying tests of manganese dust under different conditions and zinc removal from dried dust in sintering experiments. On the basis of drying tests, an empirical relationship correlating the moisture content and drying time with temperature and sample thickness was derived. The effects of sintering time, temperature, moisture content and thickness of a sample on zinc removal in sintering experiments have been established.

KEY WORDS: ferromanganese; manganese furnace dust; zinc removal; drying; sintering.

## 1. Introduction

Recycling of metallurgical wastes including dust and sludge formed in cleaning of the effluent gas is one of the most urgent issues for metallurgical industries. These dusts contain valuable elements which, when recycled, decrease consumption of raw materials and more importantly, eliminate potentially harmful by-product stockpiles. The Tasmanian Electro Metallurgical Company (TEMCO), Australia, produces ferromanganese and silicomanganese alloys in submerged arc furnaces. Manganese ores are reduced by coke and coal in the furnaces. Electricity supplies the energy for smelting and reduction reactions. Manganese dust, which contains metal oxides, volatiles and tar, is collected from the furnace off-gas wet scrubbers and then is deposited in settling ponds. The water content of the manganese dust is close to 60 mass%.<sup>1)</sup> Therefore, the dust needs to be dried before recycling. The manganese furnace dust contains up to 1.5 mass% of zinc (dry basis)<sup>1)</sup> which has to be removed prior to recycling into the smelting furnaces to avoid irregular charge movement, and potential explosions, resulting from zinc accumulation. Reduction of zinc oxide in the manganese furnace dust with tar was studied in work,<sup>2)</sup> which reported the effects of temperature and gas atmosphere. It was established that zinc oxide in the manganese furnace dust can be reduced and removed by tar under appropriate reducing conditions. The behaviour of zinc in pilot-plant sintering of manganese ore with addition of manganese furnace dust has also been examined.<sup>3)</sup> The low degree of zinc removal was attributed to reoxidation of zinc vapour and its deposition in the sinter bed.

Development of industrial technology for the manganese dust recycling requires knowledge of dust drying condi-

tions. The focus of this study is on the drying of manganese furnace dust and the removal of zinc from dried dust during sintering.

## 2. Experimental

The composition of manganese furnace dust (dry basis) is shown in **Table 1**. The drying tests were conducted in a muffle furnace at 423 to 973 K in air with a flow rate of 2 000 cm<sup>3</sup>/min. The dust sample was held in a tray of aluminium foil. The shape of a sample was rectangular with 60 mm×60 mm base and thickness of 10 to 50 mm. The sample temperature was measured by a thermocouple of which tip was placed 2 mm from the sample surface. The change of sample temperature was logged by a personal computer during a drying process.

The dust sample was set into a muffle furnace at the experimental temperature and dried for a certain time. After the experiment, the sample was taken out from the furnace and quenched on a water-cooled iron plate. The initial and final weights of the dust sample were recorded. The change in water content was calculated from the initial water content of manganese dust, which was 58.2 mass%, for different experimental temperatures, sample thicknesses and drying times. A sample temperature was 373 K during drying until most of water was removed, although the furnace temperature was in the range from 423 to 973 K. Evaporation

**Table 1.** Composition of manganese dust (mass%).

Water content before drying (wet basis)	Composition of dried dust		
	C	Mn	Zn
58.2	19.2	27.3	0.62

of volatiles during this period was negligible.<sup>1)</sup> The weight changes of samples fully dried at 423–973 K were within 1.5% relative to 383 K, showing that weight loss due to evaporation of volatiles was insignificant.

Dry-basis water content, or moisture content, was defined as the ratio of the mass of water to the mass of dry material in a sample.

Sintering tests were carried out in a muffle furnace at temperatures between 1 373 and 1 573 K. Before a sintering test, dust samples were dried for different durations at different temperatures. The thickness of a sample was also changed. The dried dust sample was put on a mullite plate (100 mm×100 mm×15 mm) and set in a furnace under air atmosphere. After sintering, the dust sample was taken out from the furnace, cooled, crashed and then digested into HNO<sub>3</sub> solution (66 vol%). Zinc content in the solution was determined by ICP-AES. The initial and final masses of zinc in a sample were calculated using the weight and chemical analysis data. The zinc removal was defined as [(Mass of initial zinc)–(Mass of final zinc)]/(Mass of initial zinc).

### 3. Results

#### 3.1. Drying Test

In drying tests, change in water content in manganese furnace dust and the surface temperature of the dust sample during drying were measured. **Figures 1 and 2** present the results obtained for a rectangular sample with drying surface area of  $3.6 \times 10^{-3} \text{ m}^2$  and a thickness of 20 mm. The initial weight of this sample was 102.5 g. The drying process can be divided into three stages. In the first, pre-heating stage, the mass of water in a sample decreased slowly with time while the sample temperature gradually increased. The duration of this first stage decreased quickly with increasing furnace temperature (Fig. 1). In the second stage, the mass of water in a sample decreased about linearly with time, while the temperature of the sample remained constant. In the current study, the drying tests were conducted under atmospheric pressure, and the observed constant temperature in Fig. 2 was very close to 373 K, the boiling point of water. In the final stage of the drying process, the temperature of the sample quickly increased to the furnace temperature, while the water content decreased with time.

#### 3.2. Sintering Test

##### 3.2.1. Effect of Sintering Time

Sintering experiments were carried out to investigate zinc removal from dried samples under different conditions. It was established in the drying experiments that the tar ignites at 433 K. To avoid loss of tar, samples were dried under such conditions that the tar ignition temperature was not achieved. When the furnace temperature was above 433 K, this was regulated by the drying time. The relationship between zinc removal and sintering time at 1 573 K is shown in **Fig. 3**. The initial thickness of the dust samples was 20 mm. Prior to sintering, samples were either fully dried at 423 K or partially dried at the furnace temperature of 873 K for 1 200 s. A sample temperature in drying experiments at furnace temperature of 873 K was controlled to be

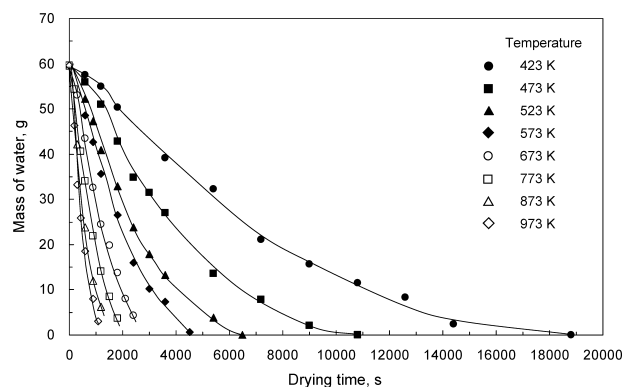


**Fig. 1.** Drying of manganese dust at different temperatures. Sample thickness was 20 mm, surface area  $3.6 \times 10^{-3} \text{ m}^2$ .

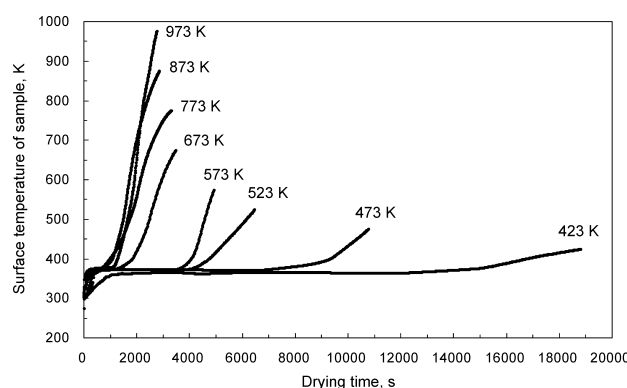


**Fig. 2.** Surface temperature of samples of manganese furnace dust in process of drying at different temperatures.

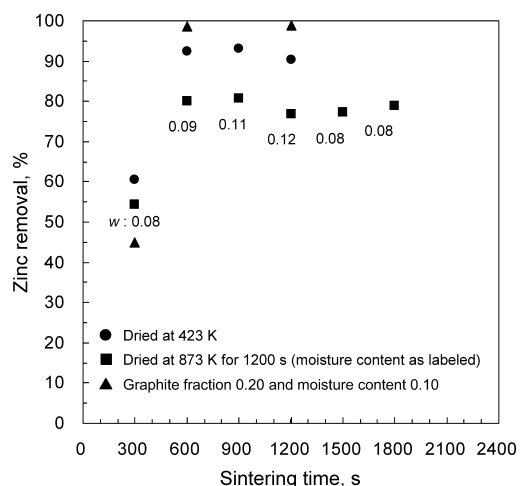


**Fig. 3.** Zinc removal in process of sintering of manganese dust at 1 573 K. The initial thickness of samples was 20 mm.

below 433 K, which avoided ignition of tar in the dust.

After sintering for 300 s, the fully dried samples shrank and were sintered 4 to 5 mm from the surface. Sintering depth increased to 5 to 6 mm after sintering for 600 s, and further to 6 to 7 mm after sintering for 900 to 1 200 s. After sintering for 300 s, the zinc removal was 61%; it achieved more than 90% after 600 s sintering and did not change with further sintering at this temperature.

Samples dried at 873 K for 1 200 s had in average a moisture content of 0.1. They were sintered to 3 to 4 mm from the surface after 300 s, and 5 to 6 mm after 600 to 1 200 s sintering. The samples shrank from original thickness of

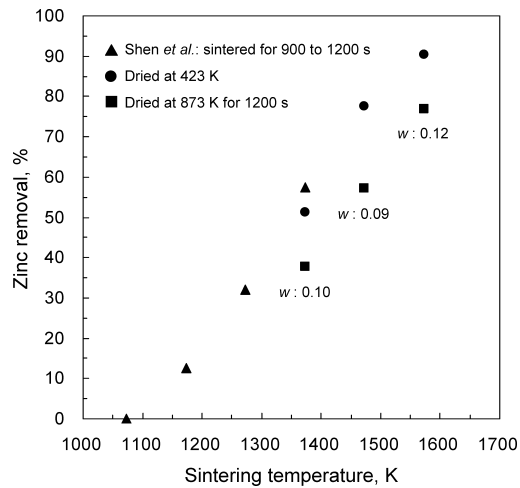


**Fig. 4.** Effect of the sintering temperature on zinc removal. Samples with initial thickness of 20 mm were sintered for 1 200 s.

20 mm to 11 to 12 mm after 1 500 to 1 800 s. The zinc removal from a sample sintered for 300 s was 51%; it increased to 80% after sintering for 600 s, and practically did not change with further sintering. The zinc removal from a fully dried sample was about 10% higher than that from a sample dried at 873 K for 1 200 s.

### 3.2.2. Effect of Sintering Temperature

Zinc removal after sintering at different temperatures is shown in **Fig. 4**. The initial thickness of the sample in these experiments was 20 mm and the dust was fully dried at 423 K or partially dried at 873 K for 1 200 s before sintering. Sintering time for all samples was 1 200 s. At 1 673 K, the sample melted and reacted with the mullite plate. The depth of sintering of samples at 1 373 and 1 473 K was about 5 mm from the surface.

Figure 4 also shows data obtained by Shen *et al.*<sup>2)</sup> by sintering pellets of dried manganese furnace dust in a muffle furnace on an alumina plate (initial Zn content was 1.5 mass%) for 900 to 1 200 s. Results from Shen *et al.*<sup>2)</sup> and this work showed a very consistent effect of temperature on the zinc removal from dried dust, although the weights and shapes of samples in the two works were different. Zinc removal increased with temperature between 1 073 and 1 573 K. The zinc removal for samples dried at 873 K for 1 200 s before sintering was about 10% lower than that for fully dried samples at 423 K, which is consistent with data in Fig. 3.

### 3.2.3. Effect of Moisture Content in Manganese Furnace Dust

Effect of moisture content of a sample on the zinc removal is shown in **Fig. 5**. The initial thickness of the sample was 20 mm; the dust was dried at either 423 K or 873 K for various durations to attain targeted moisture contents. The samples were sintered at 1 573 K for 1 200 s. The dust sample shrank but retained a rectangular shape after sintering. The depth of sintering was not visibly affected by the moisture content in the range examined. Increasing moisture content to about 20% had an insignificant effect on zinc removal. When initial moisture content of a sample

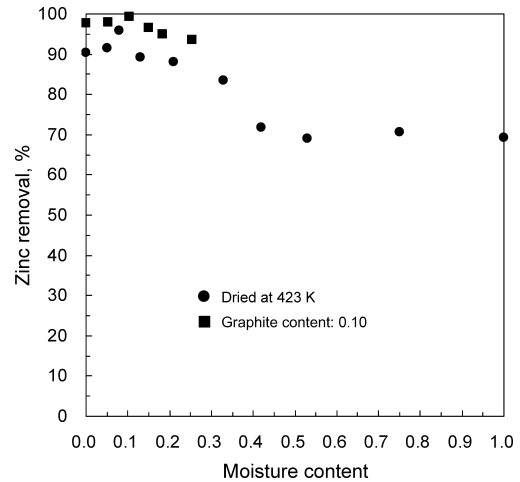


**Fig. 5.** Effect of the initial moisture content on zinc removal. Samples with initial thickness of 20 mm were sintered at 1 573 K for 1 200 s.

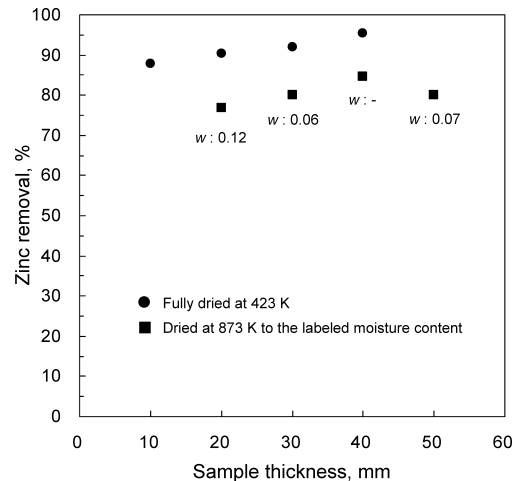


**Fig. 6.** Relationship between zinc removal and the initial thickness of samples. The samples were sintered at 1 573 K for 1 200 s.

was 0.21 (0.18 wet-basis), zinc removal was 88%. The zinc removal decreased with further increasing moisture content up to 0.53 (0.35 wet-base) and did not change with further increase in moisture. When initial moisture content was 1.00, *i.e.* 50% water content, 69% of zinc in the manganese dust was removed by sintering at 1 573 K for 1 200 s.

### 3.2.4. Effect of Thickness of Manganese Furnace Dust Sample

The relationship between zinc removal and initial thickness of a sample is shown in **Fig. 6**. The dust samples were fully dried at 423 K and then sintered at 1 573 K for 1 200 s. The sample with 10 mm thickness was almost fully sintered but interior of others was not sintered after 1 200 s. A sample with 40 mm thickness cracked and was broken; as a result it was sintered. Other samples also cracked and shrank, but they kept the rectangular shape. The depth of sintering was 6 to 7 mm from the sample surface. The zinc removal tends to increase with increasing sample thickness.

Several dust samples were dried at 873 K. To maintain similar moisture contents, the drying time was increased with increasing thickness of the sample; it was 1 800 s for a

30 mm thick sample, 2400 s for a 40 mm sample, and 3000 s for a 50 mm sample. The sintered layer at surface was 5 to 6 mm thick regardless of the initial thickness of the dust specimens. The zinc removal of these partially dried samples was about 10% lower than that of corresponding fully dried samples. This difference in the zinc removal, caused by changed drying temperature and degree of drying, was consistent with the data presented in Fig. 3. Similar to fully dried samples, the effect of sample thickness on zinc removal was small.

### 3.2.5. Effect of Additional Carbon

The effect of carbon addition to manganese furnace dust on zinc removal was also investigated. The manganese furnace dust and graphite powder ( $<20\ \mu\text{m}$ ) were intimately mixed and dried at 423 K for different times to obtain samples with different moisture contents.

Zinc removal from a manganese furnace dust-graphite mixture sintered at 1573 K for different times is shown in Fig. 3. The manganese furnace dust had a moisture content of 0.1, and the mass fraction of graphite in the dust-graphite mixture was 0.2. The initial sample thickness was 20 mm. After sintering for 300 s, the dust-graphite sample did not shrink; the sintering depth was 1 to 2 mm. The sintering depth slightly increased (to 2 mm) and the sample shrank by 5 mm after 600 s sintering. The sample shrank further to 10 mm with increasing sintering time to 1200 s, but the sintering depth did not change; the sample interior was not sintered. The zinc removal was 45% after 300 s sintering, increased to 99% after 600 s and did not change with further sintering. Compared to samples without added graphite, the zinc removal increased by 6 to 8% in sintering of a fully dried dust sample for 600 s or longer, and by about 20% in sintering of the dust dried at 873 K for 1200 s and having similar moisture content.

The zinc removal from a manganese furnace dust-graphite mixture with different moisture contents is shown in Fig. 5. In these experiments, graphite mass fraction in the dust-graphite mixture was 0.1; the initial sample thickness was 20 mm. The samples were sintered at 1573 K for 1200 s. The zinc removal from fully dried samples was 98%, and decreased slightly with increasing moisture content. Adding graphite enhanced zinc removal by 6 to 8%.

**Figure 7** shows the relationship between zinc removal and graphite content in the dust-graphite mixture. The samples were dried at 423 K before sintering. The moisture content of the dust was 0.10 and the initial thickness of the mixture was 20 mm. Sintering was carried out at 1573 K for 1200 s. The zinc removal was 94% when the graphite mass fraction was 0.05. It reached 99% with increasing carbon content to 0.10 and more.

## 4. Discussion

It is well established<sup>4,5</sup> that drying of wet materials consists of three stages as schematically presented in **Fig. 8**: a short preheating stage, a constant drying rate stage and a final staged with decreasing drying rate. In the preheating stage, the temperature of the wet material,  $T_m$ , rapidly increases approaching the boiling temperature while the decrease of moisture content,  $w$ , is not significant. Then, the

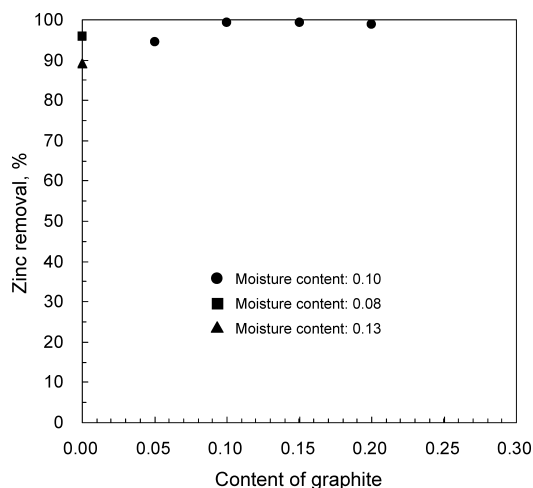


**Fig. 7.** Effect of addition of graphite on zinc removal. Sample thickness was 20 mm. Sintering was carried out at 1573 K for 1200 s.

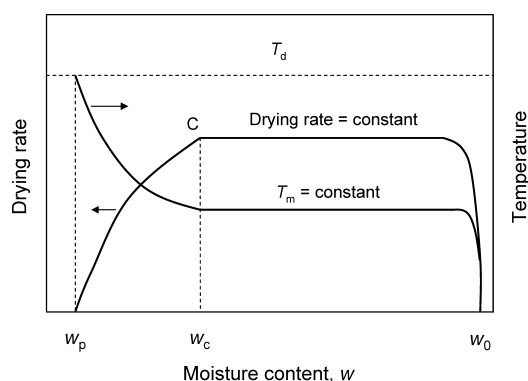


**Fig. 8.** Change of drying rate and material temperature with moisture content.

material temperature becomes stabilised at near the boiling temperature. In this period, heat delivered to the material is consumed for the evaporation of water from the surface. The drying rate is controlled by the rate of water evaporation while water flow to the surface has negligible resistance. The surface temperature and drying rate during this period are constant. When the moisture decreases to a level presented by point C in Fig. 8, the water mass transfer from interior to the surface offers significant resistance, the drying rate starts to decrease and the surface temperature starts to increase. This last stage lasts until the moisture content decreases to  $w_p$ , when the material temperature approaches drying temperature  $T_d$ .

The position of critical point C in Fig. 8 changes with drying conditions. The constant drying rate stage is not clearly seen in Fig. 1 due to the scattering of experimental data, however its existence follows from experimental data in Fig. 2 which shows a constant surface temperature period in all experimental tests. This stage becomes shorter with increase in drying temperature.

Time required for complete drying of a dust sample,  $t_c$ , was determined from the drying curves (Fig. 1). For the drying experiments at 423 to 573 K, over 99% of water being removed, the  $t_c$  values were directly found from the drying curves. The  $t_c$  values at 673 to 973 K were estimated by extrapolation of the drying curves in Fig. 1. The  $t_c$  values at 423 K for samples with different thickness are shown

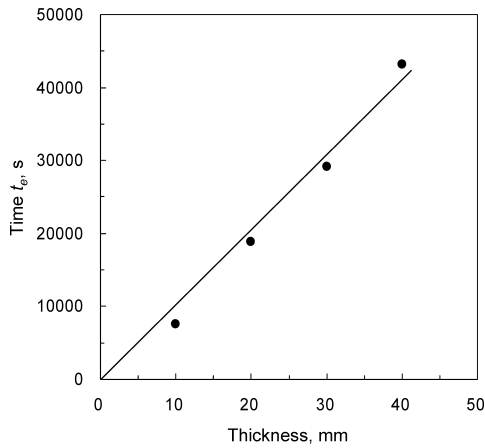


Fig. 9. Time needed to fully dry dust samples of different thickness at 423 K.

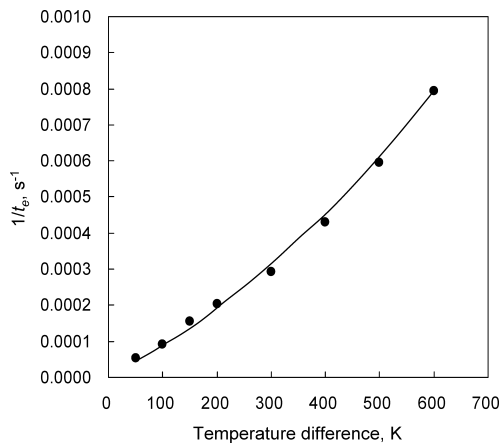


Fig. 10. Time needed to fully dry a 20 mm thick sample at different temperatures. Difference between the furnace and sample temperatures is taken at drying stage with constant rate.

in Fig. 9. At a fixed drying temperature,  $t_e$  was directly proportional to the thickness of the sample.

Figure 10 shows the change of reciprocal of complete drying time with the furnace–sample temperature difference (at the constant surface temperature period) for a sample 20 mm thick. The relationship can be presented by Eq. (1).

$$\frac{1}{t_e} = 9.0 \times 10^{-10} (T_d - T_m)^2 + 7.6 \times 10^{-7} (T_d - T_m) \dots(1)$$

Therefore, the time needed to fully dry a sample with a thickness of  $z$  mm can be calculated by Eq. (2).

$$t_e = \frac{z}{1.8 \times 10^{-8} (T_d - T_m)^2 + 1.5 \times 10^{-5} (T_d - T_m)} \dots(2)$$

The dimensionless time,  $\tau$ , was defined as the ratio of drying time,  $t$  and the time needed to fully dry the dust:

$$\tau = \frac{t}{t_e} \dots(3)$$

A plot of moisture content (which is dimensionless) against dimensionless time under different drying tempera-

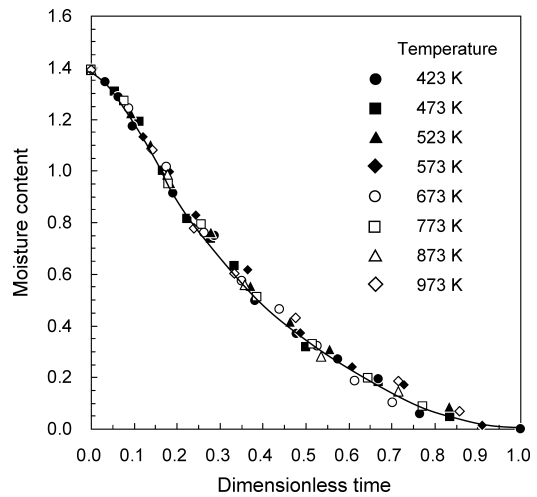


Fig. 11. Relationship between the moisture content in the manganese dust and dimensionless time.

tures is presented in Fig. 11. Ignoring the different stages of drying, the experimental points in the figure can be approximated by a polynomial formula:

$$w = 8.50 \tau^5 - 23.4 \tau^4 + 22.7 \tau^3 - 7.71 \tau^2 - 1.53 \tau + 1.40 \dots(4)$$

Duration of the constant temperature period estimated from the results of temperature measurement (Fig. 2) and  $t_e$  at each drying temperature was found from 0.17 to 0.57 (dimensionless time). Experimental data on the rate of water removal in this period are not described by the linear function due to scattering of experimental data, however, the plot is linear in the  $\tau$  range 0.17–0.39:

$$w = -2.30 \tau + 1.39 \dots(5)$$

When the temperature gradient inside drying material layer is small (except of the decreasing drying rate stage), the material temperature can be considered uniform and equal to  $T_m$ . Heat balance for the dust drying process can be presented by Eq. (6).<sup>6)</sup>

$$-\frac{dW}{dt} r_w + (m_0 C_0 + W C_w) \frac{dT_m}{dt} = hA(T_d - T_m) \dots(6)$$

Where  $W$  is mass of water in a sample;  $t$  is the drying time;  $r_w$  is the latent heat of water evaporation (2 270 kJ/kg at 373 K);  $m_0$  is the mass of dried material;  $C_0$  and  $C_w$  are the specific heat capacities of dried material and water, respectively;  $h$  is the heat transfer coefficient; and  $A$  is the drying surface area of a sample.

In constant drying rate stage when a sample temperature is constant, the heat supplied to the sample is equal to the heat of water evaporation. Therefore,

$$-\frac{dW}{dt} r_w = hA(T_d - T_m) \dots(7)$$

The drying rate during these periods of constant sample temperature can be used to assess the heat transfer coefficient in Eq. (7).

The constant drying rate,  $R_c$  can be calculated using Eq.

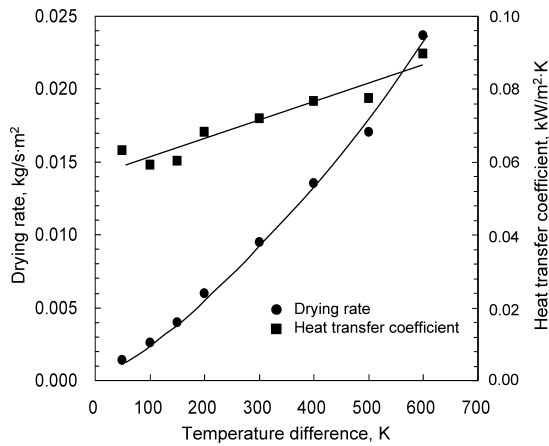


Fig. 12. Rate constant and heat transfer coefficient in the process of dust drying at different temperatures. Difference between the furnace and sample temperatures is taken at drying stage with constant rate.

(8) and heat transfer coefficient by Eq. (9):

$$R_c = -\frac{1}{A} \frac{dW}{dt} \dots\dots\dots(8)$$

$$h = \frac{R_c r_w}{T_d - T_m} \dots\dots\dots(9)$$

Values of  $-dW/dt$  were found from the slopes of drying curves, averaged over time when the sample temperature was constant. The constant drying rate and heat transfer coefficient are plotted against the temperature difference,  $(T_d - T_m)$ , in Fig. 12 where  $T_m$  is supposed to be 373 K. The error of the calculated drying rate in the constant drying period was within  $\pm 8.5\%$ . The heat transfer coefficient can be described by the following equation:

$$h = 5.0 \times 10^{-5} (T_d - T_m) + 0.056 \dots\dots\dots(10)$$

The increase of the heat transfer coefficient with increase in temperature difference is attributed to the enhanced natural convection and stronger radiation heat transfer at higher drying temperatures.

The effect of moisture content on the zinc removal from the samples dried at low temperature of 423 K was small when the moisture content was less than 0.21 (Fig. 5). When the dust was dried at 873 K for 1 200 s, the moisture content was 0.08 to 0.12. However, the zinc removal from samples dried at 873 K for 1 200 s was about 10% lower than from samples dried at 423 K. In sintering experiments, zinc oxide was reduced by carbon of tar in the manganese furnace dust. Shen *et al.*<sup>1)</sup> reported that the tar mainly consists of C<sub>15</sub>–C<sub>28</sub> aliphatic and polyaromatic hydrocarbons with boiling points in the range of 503–803 K and molecular weights of 150–400. Under drying conditions in this work, the dust temperature was controlled to be below the ignition temperature of the tar. However, this does not prevent loss of some more volatile tar components, even though the boiling points of the tar components are high. The carbon content of the dust before sintering was determined by LECO carbon and sulphur analyser. The carbon content of the sample fully dried at 423 K was 19.2 mass%.

The dust dried at 873 K for 1 200 s contained 17.2 mass% of carbon. About 2 mass% of carbon was lost during drying at 873 K. Although the zinc oxide concentration in the fully dried dust sample is small (0.62 mass% Zn), and carbon content in the dust was well above the level needed for zinc oxide reduction, it is essential to have carbon in excess to maintain highly reducing atmosphere in the sample interior to avoid re-oxidation of zinc vapour formed by reduction. This can also explain the increase in zinc removal with addition of graphite. However, this effect is not strong and does not justify additional cost associated with usage of additional carbonaceous materials.

5. Conclusions

The drying of the manganese furnace dust was studied at 423 to 873 K. The majority of the water was removed during constant temperature drying period when the sample temperature was close to 373 K. Drying time was directly proportional to the sample thickness and decreased with drying (furnace) temperature. Tar ignites at 433 K; to avoid carbon loss, dust was dried under controlled conditions, so that the sample temperature was below the ignition temperature. The empirical relationship between dimensionless moisture content and drying time was established which allows prediction of the moisture content based on the drying temperature, sample thickness and drying time.

The sintering tests of the manganese furnace dust were carried out at 1 373 to 1 573 K. The zinc removal from dried dust samples under controlled conditions increased with increasing sintering temperature. At 1 573 K, zinc removal increased with increasing sintering time to 600 s, and practically did not change with further sintering. Sintering of a sample with 20 mm initial thickness was not completed at 1 573 K after 1 200 s. This did not affect zinc removal. The moisture content of a dried sample up to  $w=0.21$  had little influence on zinc removal. Zinc removal decreased with increasing moisture content up to  $w=0.53$  and did not change at higher moisture contents. Zinc removal from a sample dried at 873 K was about 10% lower than that from a sample dried at 423 K to the similar moisture content. A 10 mass% addition of graphite powder to the manganese furnace dust increased the zinc removal by 6 to 8% at 1 573 K. When graphite mass fraction in the dust–graphite mixture was above 0.10, the zinc removal was 99% at 1 573 K ( $w=0.10$ ).

REFERENCES

- 1) R. Shen, G. Zhang, M. Dell’Amico, P. Brown and O. Ostrovski: *ISIJ Int.*, **45** (2005), 1248.
- 2) R. Shen, G. Zhang, M. Dell’Amico, P. Brown and O. Ostrovski: *ISIJ Int.*, **46** (2006), 8.
- 3) R. Shen, G. Zhang, M. Dell’Amico, P. Brown and O. Ostrovski: *ISIJ Int.*, **47** (2007), 234.
- 4) G. Jin *et al.* (ed.): *Drying Equipment*, Chemical Industry Press, Beijing, China, (2002), 34 (in Chinese).
- 5) C. Yu, B. Wang and X. Wang (ed.): *Handbook of Drying Plant Designs*, Chemical Industry Press, Beijing, China, (2005), 22 (in Chinese).
- 6) M. Nakamura and Y. Tatemoto: *Kansogijutsu*, Kogyo Chosakai Publishing Inc., Tokyo, Japan, (2005), 133, 194 (in Japanese).